

Supplementary Information

MATERIALS AND METHODS

Generation of CD3 multicistronic vectors

CD3 multicistronic constructs were generated as described previously (Holst *et al.*, 2006a; Holst *et al.*, 2006b; Holst *et al.*, 2008). Briefly, 2A peptide-linked CD3 constructs were generated by recombinant PCR and cloned into pMIG, an MSCV-based retroviral vector containing an IRES-GFP cassette. The lysines on 2A peptides were mutated to arginines without altering 'self-cleaving' capability (data not shown). The lysines on the cytoplasmic domain of each CD3 chain were mutated to arginines by recombinant PCR and subsequent CD3 mutant constructs were then generated by appropriate subcloning.

Generation of retroviral producer cells

Retroviral producer cell lines were generated as described previously (Holst *et al.*, 2006a; Holst *et al.*, 2006b; Holst *et al.*, 2008). Briefly, HEK-293T cells were transiently transfected with CD3 multicistronic vectors (4 µg), together with packaging and envelope vectors using TransIT LT1 transfection reagent (Mirus). The supernatant containing virus was collected and used to transduce GP+E86 cells in the presence of polybrene (6 µg/ml) every 12 h for 3-4 days until a viral titer greater than 10^5 /ml after 24 h was obtained.

Flow cytometric analysis, intracellular staining and cell sorting

Thymocytes were purified by FACS using mAbs against CD4 and CD8, with or without CD69 mAb (BD-PharMingen). Splenic T cells and B cells from C57BL/6J mice were purified by FACS using TCRβ and B220 mAbs. Peripheral T cells from the spleens and lymph nodes of C57BL/6J or retrogenic mice

were purified by negative MACS (AutoMACS; Miltenyi Biotec). Following red blood cell lysis with Gey's solution, cells were stained with biotinylated mAbs against Mac1, Ter119, Gr1, B220, NK1.1 (BD-PharMingen), followed by streptavidin coupled magnetic beads. For flow cytometric analysis, mAbs against the following molecules were used: CD4 (RM4-5), CD5 (53-7.3), CD8 (53-6.7), CD25 (PC61), CD69 (H1.2F3), B220 (RA3-6B2), TCR β (H57), and Foxp3 (FJK-16s) (All BD-PharMingen). Flow cytometric analysis was performed using a FACSCalibur (Becton Dickinson).

CD3 ϵ crosslinking and intracellular staining

Bulk thymocytes were plated at 2×10^6 cells per well in 96 well flat bottom plate and rested for 1 hour at 37°C in 0.5% FCS RPMI. After resting, MEK inhibitor was added at a final concentration of 10 μ M U0126 (Sigma) in 0.1% DMSO to medium or thymocytes were treated with 0.1% DMSO only (Vehicle). Cells were fixed in 4% final Formaldehyde (Polysciences, Inc.) and permeablized in 95% final ice cold Methanol. Permeablized cells were stained with a pERK Ab (P-p44/42 MAPK, Cell Signaling) and detected with Alexa-647–conjugated Ab against rabbit IgG.

Lipid bilayers and microscopic analyses

Lipid bilayers were constructed essentially as described (Sumen *et al.*, 2004), with some modifications (Kaizuka *et al.*, 2007). Briefly, liposomes comprised of 90% dioleoylphosphocholine, 10% DOGS (1,2-dioleoyl-SN-Glycero-3- $\{[N(5\text{-amino-1-carboxypentyl})\text{ iminodiacetic acid}]succinyl\}$), and 0.2% biotin-CAP-PE were deposited on glass coverslips cleaned with piranha solution (50:50 mixture of 30% H₂O₂ and 96% H₂SO₄). Alexa-555-conjugated streptavidin and biotinylated TCR β mAb were sequentially loaded onto the bilayer, while unlabeled poly-his-tagged ICAM1 produced in a baculovirus system was also loaded to facilitate T cell adhesion. Sorted DP thymocytes were added to the bilayer in RPMI medium containing HEPES and 2% FBS. Cells were fixed with 4% formaldehyde following 15 min

stimulation and immediately imaged using a Zeiss 200M spinning disk confocal microscope and analyzed using Slidebook software.

RNA, cDNA and quantitative real-time PCR

RNA from sorted thymocytes, T cells or B cells was isolated using the Qiagen microRNA extraction kit following the manufacturer's instructions. RNA was quantitated spectrophotometrically and cDNA was reverse transcribed using the cDNA archival kit (Applied Biosystems) following the manufacturer's guidelines. TaqMan primers and probes were designed with PrimerExpress software and synthesized in the St. Jude Hartwell Center for Biotechnology and Bioinformatics:

CD3 δ 5' primer, AAAGGTGGTGTCTTCTGTGCAA;

CD3 δ 3' primer, CCCGAGTCTAGCTCCACACAGT;

CD3 δ probe, FAM-TCCATTACCGAATGTGCCA.

CD3 γ 5' primer, GCGGGACAGGATGGAGTTC;

CD3 γ 3' primer, TTCATTTTGCAACAGAGTCTGCTT;

CD3 γ probe, FAM-CCAGTCAAGAGCTTCAGA.

CD3 ϵ 5' primer, CAGCCTCAAATAAAAACACGTA CTG;

CD3 ϵ 3' primer, TCAGGTCCACCTCCACACAGT;

CD3 ϵ probe: FAM-CTGAAAGCTCGAGTGTGTGA.

CD3 ζ 5' primer, GAGGAGGAACCCCCAGGAA;

CD3 ζ 3' primer: TG TAGGCTTCTGCCATCTTGTC;

CD3 ζ probe: FAM-CGTATACAATGCACTGCAG.

For quantitative analysis, an ABI Prism 7900 Sequence Detection System was used for real-time RT-PCR. Expression was normalized relative to the expression of endogenous β actin.

Transient transfection of HEK-293T cells

Transient transfection of HEK-293T cells was performed as previously described (Liu *et al.*, 2000; Szymczak *et al.*, 2004) with some modifications. HEK-293T cells were incubated in 6 well plates at 2×10^5 /plate overnight at 37°C. TCR $\alpha\beta$ (2A-linked) plasmid (1 μ g) and indicated CD3 plasmid (1 μ g) with or without a construct containing WT or a dominant negative dynamin (1 μ g) were transfected to HEK-293T cells using 6 μ l TransIT LT1 transfection reagent (Mirus). Cells were harvested 40 h after transfection and stained with CD3 ϵ and TCR β mAbs for flow cytometry analysis.

Thymic Organ Culture

Thymic organ culture was performed as previously described (D'Oro *et al.*, 1997; Hogquist, 2001; Holst *et al.*, 2008) with some modifications. The culture medium is RPMI (Gibco) buffer supplemented with 10% FBS, 50 μ M 2-mercaptoethanol, 2 mM L-glutamine, 50 U/mL penicillin, 50 mg/mL streptomycin, 50 mg/mL gentamycin sulfate, and 5 mM HEPES. Thymic lobes from newborn mice (P1) were cultured on a culture plate insert (Millipore) floating in a prepared well for 20 h at 37°C. Cultures were carried out in 1 ml of medium containing indicated reagents or vehicle control in 6-well plates. The plate was placed in a tupperware dish which has a water soaked paper towel in its bottom. Individual thymic lobes were harvested and single-cell suspensions were analyzed for surface TCR expression by flow cytometry. Following reagents were used in thymic organ culture: MG132, Lactocytin, NH₄Cl (Sigma),

Concanamycin A (Sigma), MiTMAB (EMD Chemicals Inc.), PP2 (Calbiochem), Syk inhibitor (Calbiochem), and PP1 (Invitrogen).

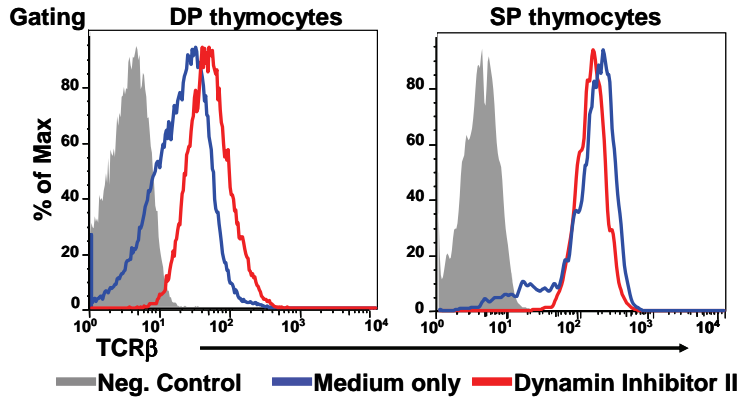
Histological examination

Histological examination was performed as previously described (Holst *et al.*, 2008). Hematoxylin and eosin stained, formalin-fixed (10% neutral buffered), paraffin-embedded tissue sections (4 μ m) of liver, lung and intestinal tract were evaluated in a blinded fashion by an experienced veterinary pathologist (Kelli Boyd, Department of Pathology, St. Jude Children's Research Hospital). Inflammation in each organ was assigned a score of 0 to 3 based on a semi-quantitative grading scheme established for this model (Supplementary Table 1).

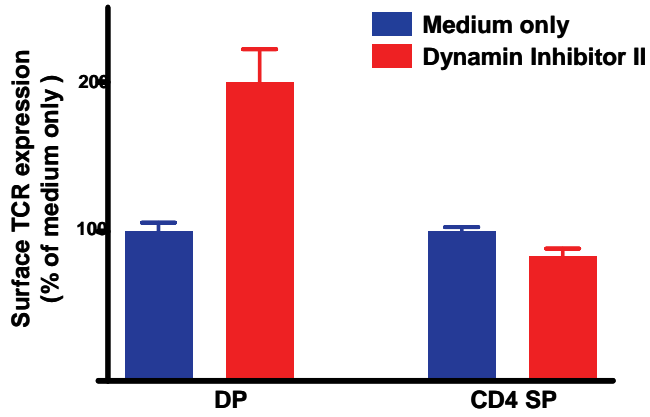
REFERENCES

- D'Oro U, Vacchio MS, Weissman AM, Ashwell JD (1997) Activation of the Lck tyrosine kinase targets cell surface T cell antigen receptors for lysosomal degradation. *Immunity* **7**: 619-628
- Hogquist KA (2001) Assays of thymic selection. Fetal thymus organ culture and in vitro thymocyte dulling assay. *Methods Mol Biol* **156**: 219-232
- Holst J, Szymczak-Workman AL, Vignali KM, Burton AR, Workman CJ, Vignali DA (2006a) Generation of T-cell receptor retrogenic mice. *Nat Protoc* **1**: 406-417
- Holst J, Vignali KM, Burton AR, Vignali DA (2006b) Rapid analysis of T-cell selection in vivo using T cell-receptor retrogenic mice. *Nat Methods* **3**: 191-197
- Holst J, Wang H, Eder KD, Workman CJ, Boyd KL, Baquet Z, Singh H, Forbes K, Chruscinski A, Smeyne R, van Oers NS, Utz PJ, Vignali DA (2008) Scalable signaling mediated by T cell antigen receptor-CD3 ITAMs ensures effective negative selection and prevents autoimmunity. *Nat Immunol* **9**: 658-666
- Kaizuka Y, Douglass AD, Varma R, Dustin ML, Vale RD (2007) Mechanisms for segregating T cell receptor and adhesion molecules during immunological synapse formation in Jurkat T cells. *Proc Natl Acad Sci U S A* **104**: 20296-20301
- Liu HY, Rhodes M, Wiest DL, Vignali DAA (2000) On the dynamics of TCR:CD3 complex cell surface expression and downmodulation. *Immunity* **13**: 665-675
- Sumen C, Dustin ML, Davis MM (2004) T cell receptor antagonism interferes with MHC clustering and integrin patterning during immunological synapse formation. *J Cell Biol* **166**: 579-590
- Szymczak A, Workman CJ, Wang Y, Vignali KM, Dilioglou S, Vanin EF, Vignali DAA (2004) Correction of multi-gene deficiency *in vivo* using a single 'self-cleaving' 2A peptide-based retroviral vector. *Nature Biotechnology* **22**: 589-594

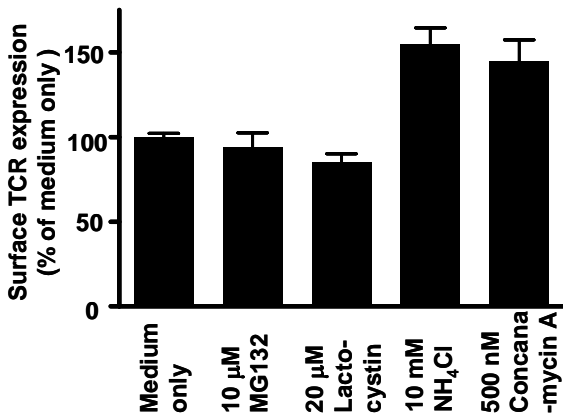
A



B

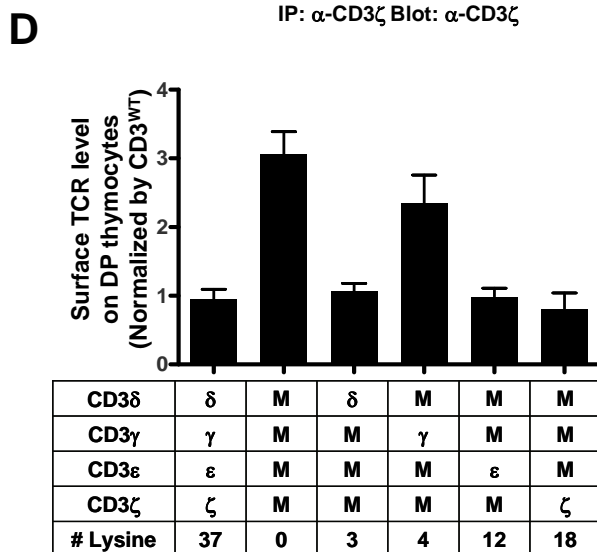
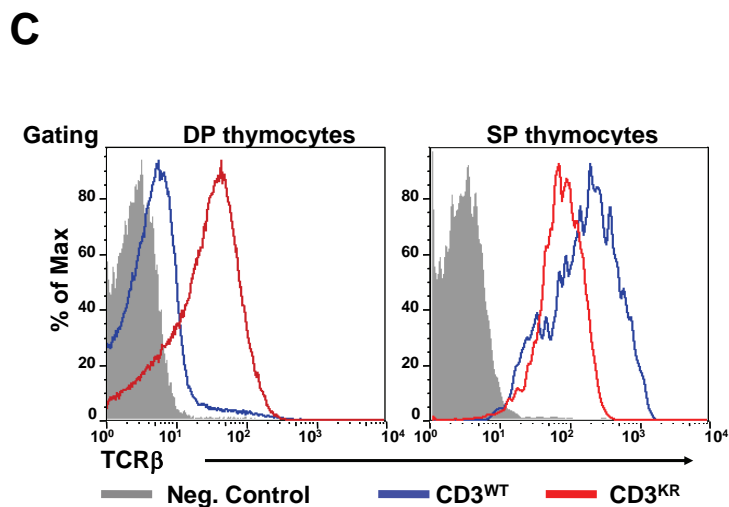
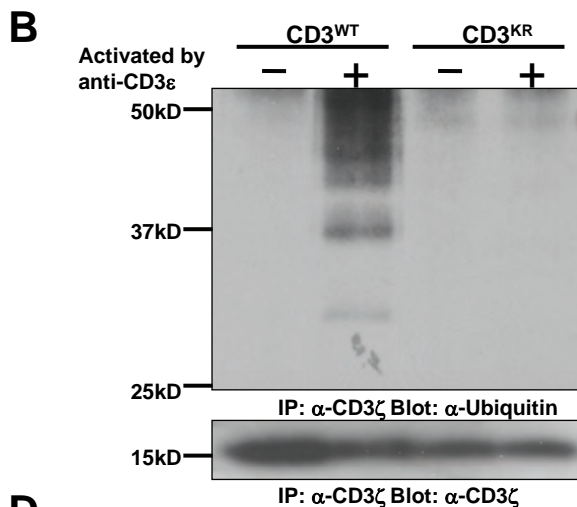


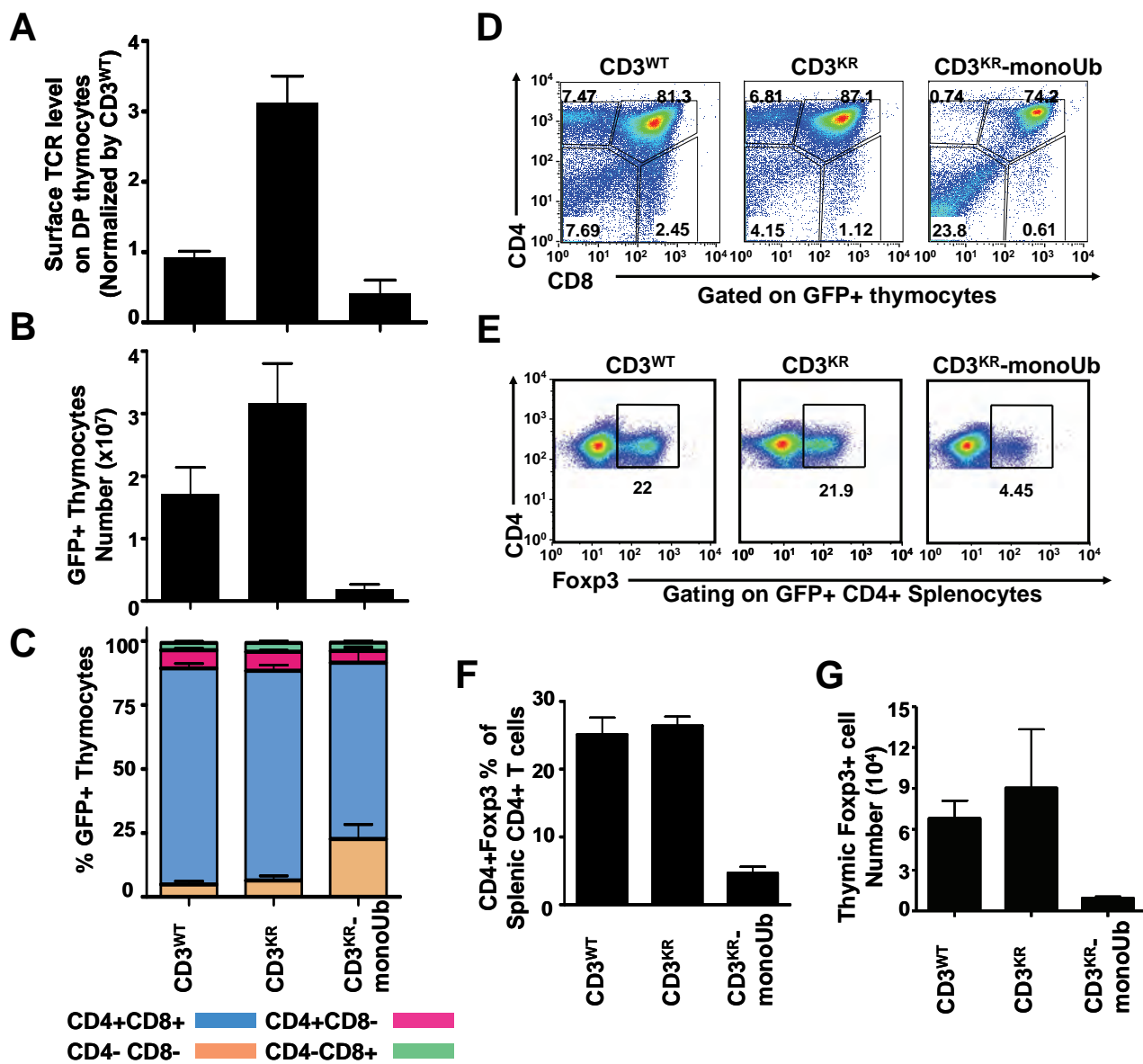
C

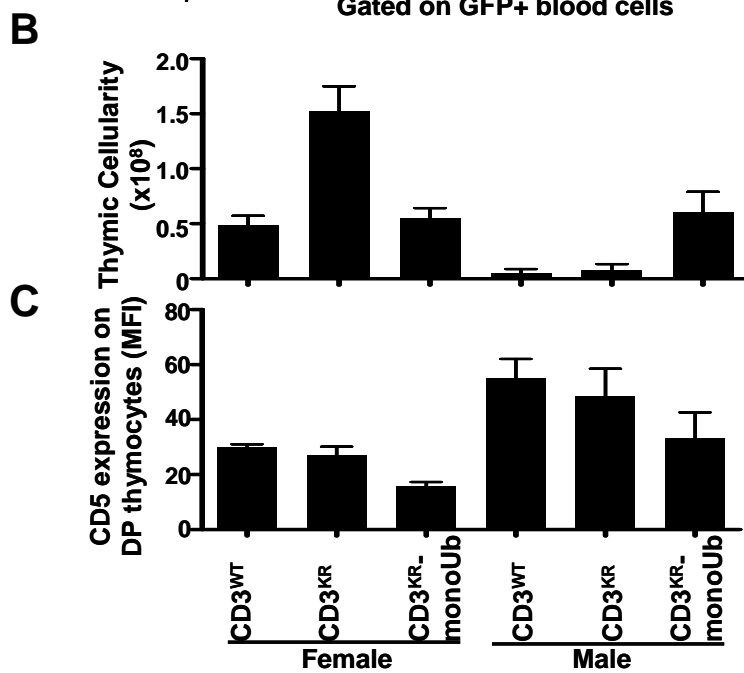
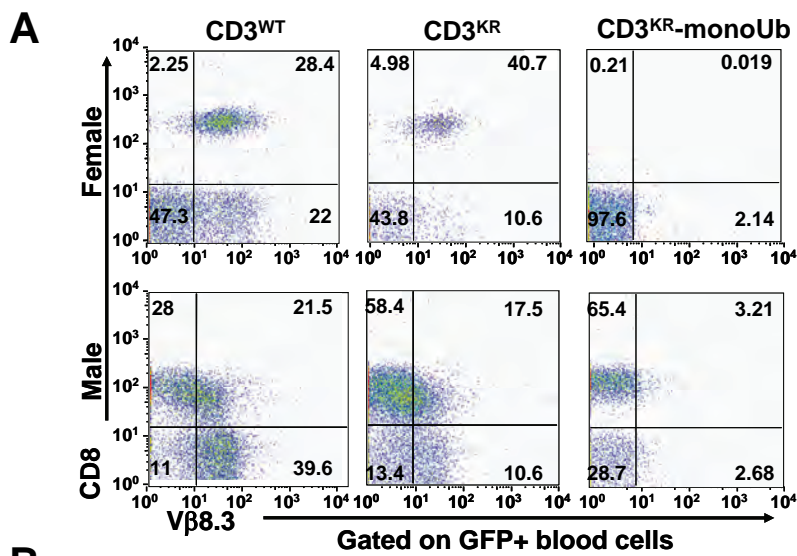


A

CD3 δ	HETGRPSGAAEVQALLKNEQLYQPLRDREDTQYSRLGGN WPRNKKS
CD3 γ	QDGVQRSRASDKQTLQNEQLYQPLKDREYDQYSHLQGN QLRKK
CD3 ϵ	SKNRKAKAKPVTRGTGAGSRPRGQNKERPPVPNPDYEP IRKGQRDLYSGLNQRV
CD3 ζ	RAKFSRSAETAANLQDPNQLYNELNLGRREEYDVLEKKR ARDPEMGGKQQRRRNPQEGVYNALQDKMAEAYSEIGTK GERRRGKGHDLGYQLSTATKDTYDALHMQLAPR







Score	Lung and Liver	Small and Large Intestine
0 (Negative)	Rare inflammatory cells in the perivascular space	Rare inflammatory cells in the perivascular space
1 (Mild)	Well delineated cuffs of inflammatory cells around vessels	Lymphocytes and plasma cells with few neutrophils and macrophages in the lamina propria, without necrosis of crypts
2 (Moderate)	Perivascular cuffing and vasculitis	Lamina propria inflammation multifocal crypt necrosis, multifocal enterocyte apoptosis, moderate dilation of lymphatics
3 (Severe)	Perivascular cuffing, vasculitis and parenchymal necrosis	Mucosal ulceration, inflammatory infiltrate in lamina propria and mucosa, wide spread crypt necrosis, transmural edema

Supplementary Table 1 | Pathology Score Description

The table describes the scale and the types of inflammation observed in those mice shown in Supplementary Fig. 7.

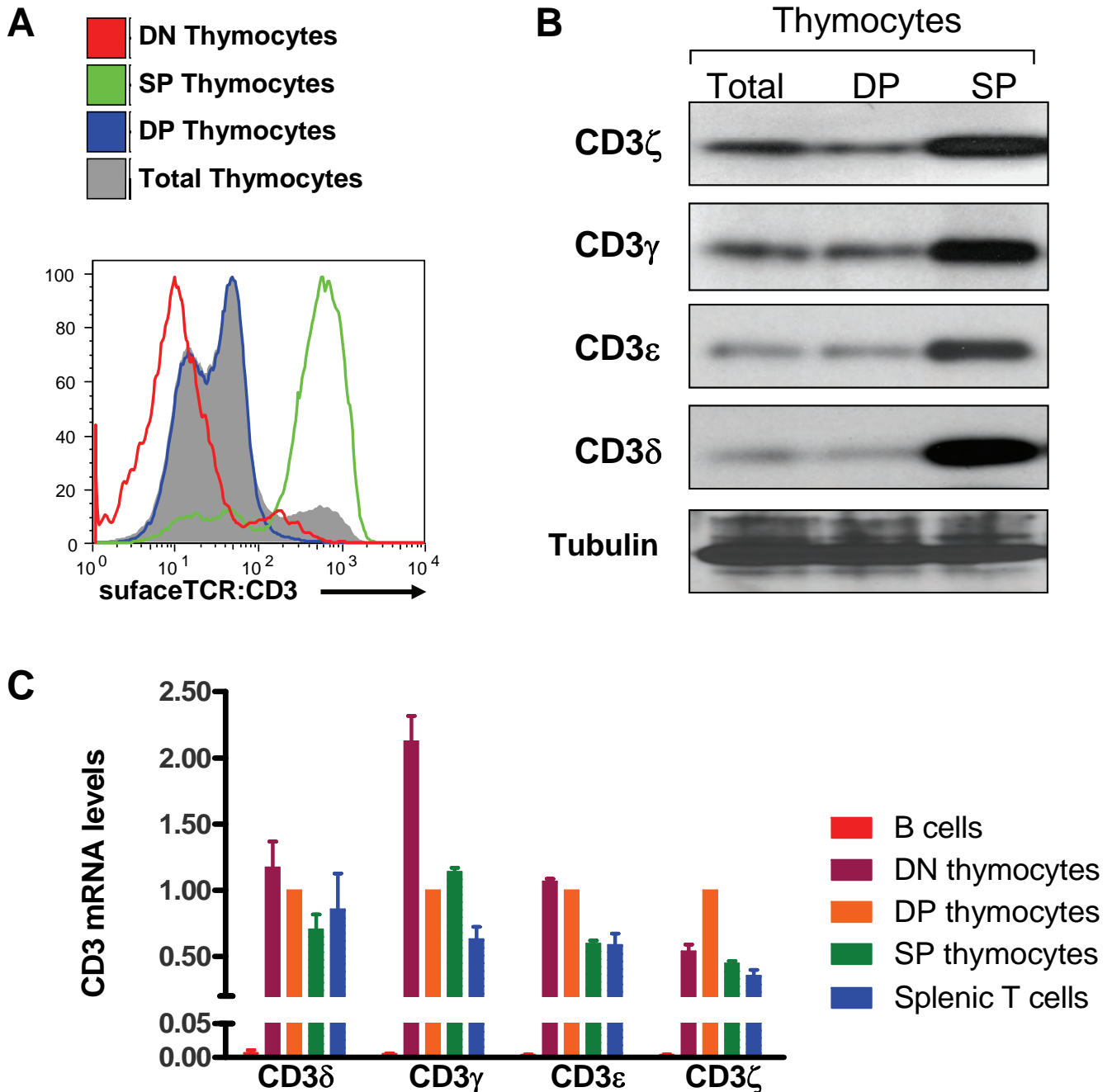


Figure S1 | Lower expression of TCR: CD3 complex on immature T cells

(A) Thymi were isolated from 6 week old C57BL/6J mice. Surface expression of the TCR:CD3 complex on DN, DP, SP and total thymocytes was measured by staining with a CD3 ϵ antibody and was analyzed by flow cytometry. (B) Thymocytes were stained with antibodies to CD4 and CD8, and DP and SP thymocytes were purified by FACS. Total, DP and SP thymocytes were lysed and an equal amount of total protein was loaded in each sample. The protein levels of CD3 δ , CD3 γ , CD3 ϵ , CD3 ζ and tubulin (loading control) were measured by SDS-PAGE and Western blot. (C) DP and SP thymocytes were purified by FACS as above. DN thymocytes were purified using Lin⁻ (CD4-CD8-B220-Mac1⁻Ter119-panNK-TCR β -TCR $\delta\gamma$ ⁻) and Thy1.2⁺ antibodies. B cells were purified from splenocytes on B220. RNA was extracted and reverse transcribed to cDNA. By using β -actin gene as an internal control, the CD3 δ , CD3 γ , CD3 ϵ and CD3 ζ mRNA levels were measured by qPCR. All data were normalized by the CD3 mRNA levels in DP thymocytes.

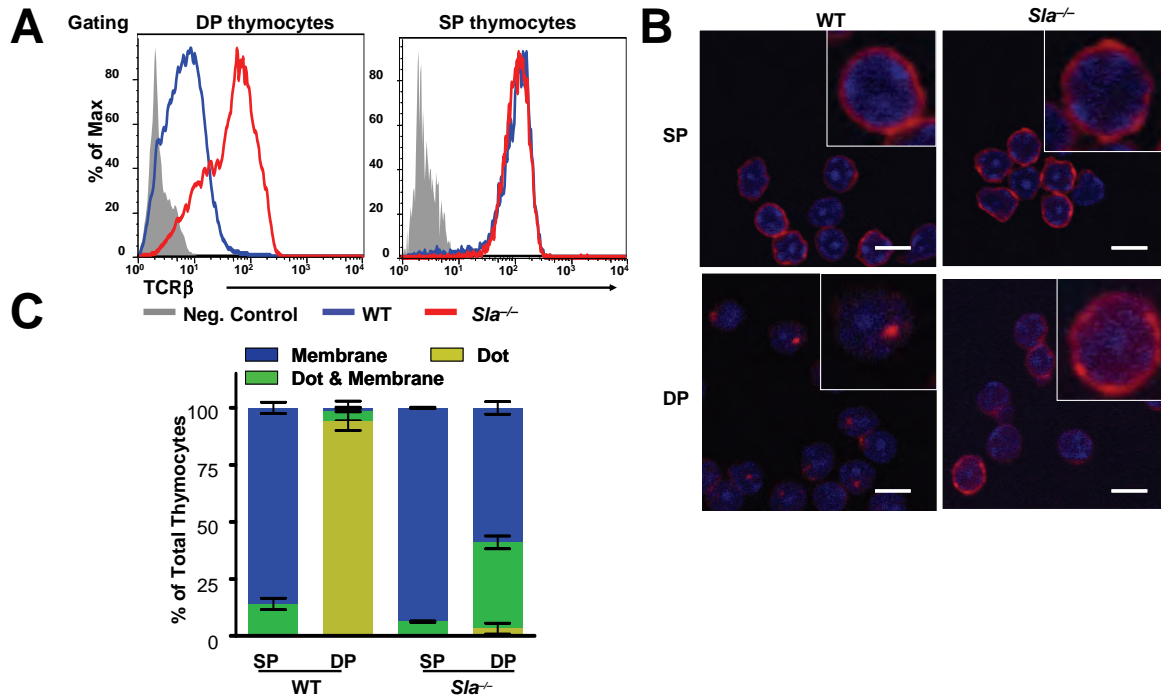


Figure S2 | SLAP is involved in the regulation of TCR expression in DP thymocytes

(A) Thymi were isolated from either C57BL/6J mice or *Sla*^{-/-} mice. Surface expression of the TCR:CD3 complex was measured by staining anti-TCR β and analyzed by flow cytometry. (B) Thymocytes were stained with antibodies to CD4 and CD8, and DP and SP thymocytes were purified by FACS. Purified thymocytes were fixed, permeabilized, and stained with a CD3 ζ antibody conjugated with Alexa-647. The localization of CD3 ζ (red) and DAPI stained nucleus (blue) are shown. (C) The distribution of CD3 ζ in the thymocyte populations indicated is shown as a bar chart.

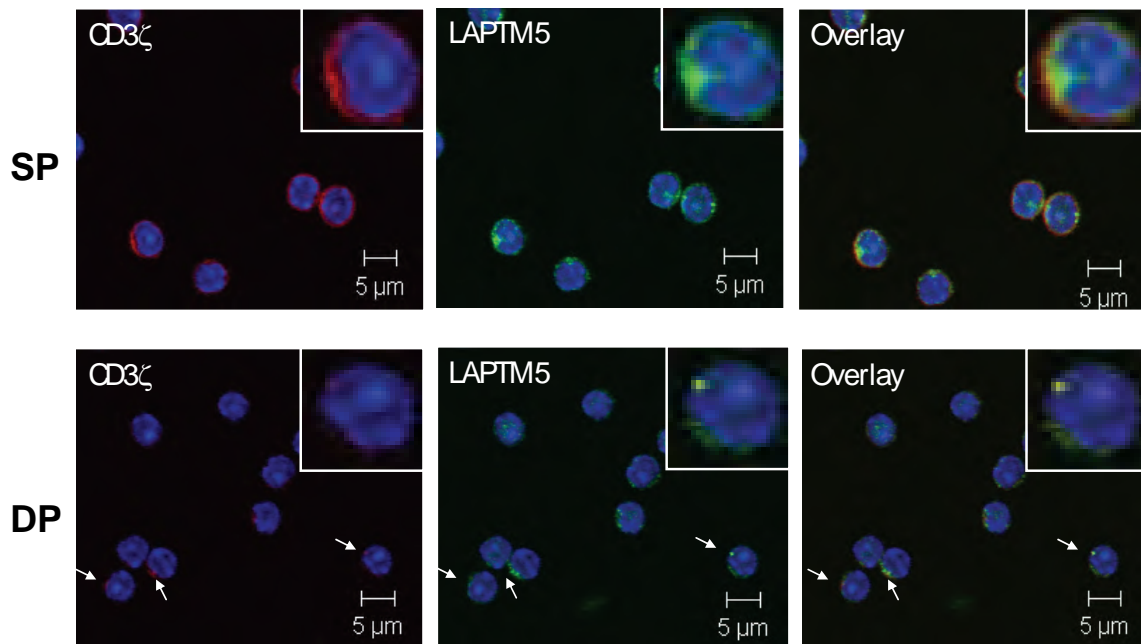


Figure S3 | Colocalization of CD3 ζ with LAPT5 in DP thymocytes .

Thymocytes were stained with antibodies to CD4 and CD8. DP and SP thymocytes were purified by FACS. Thymocytes were fixed, permeabilized, and stained with a CD3 ζ antibody conjugated with Alexa-647 and a LAPT5 antibody, which was subsequently detected with an Alexa-488-tagged rabbit IgG secondary antibody. Nuclei were stained with DAPI. The scale bar is 5 μ m.

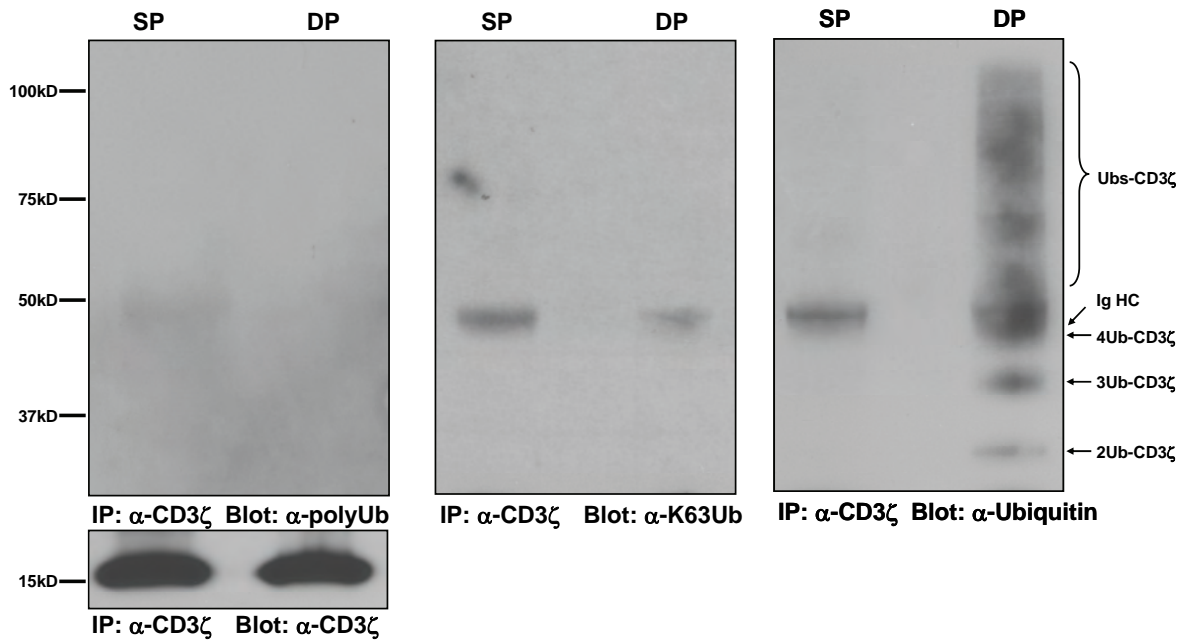


Figure S4 | Constitutive multi-mono ubiquitylation of CD3 ζ in DP thymocytes.

DP (240×10^6) and SP (30×10^6) thymocytes were purified by FACS and lysed in 1 ml lysis buffer. The lysates were immunoprecipitated with a CD3 ζ antibody (551- ζ), separated by SDS-PAGE and Western blots probed with a mAb to either polyUb (FK1, left), K63Ub (HWA4C4, middle), or Ub (P4D1, right). Blots were stripped and re-probed with anti-CD3 ζ (H146) to show that an equal amount of CD3 ζ was analyzed in each sample.

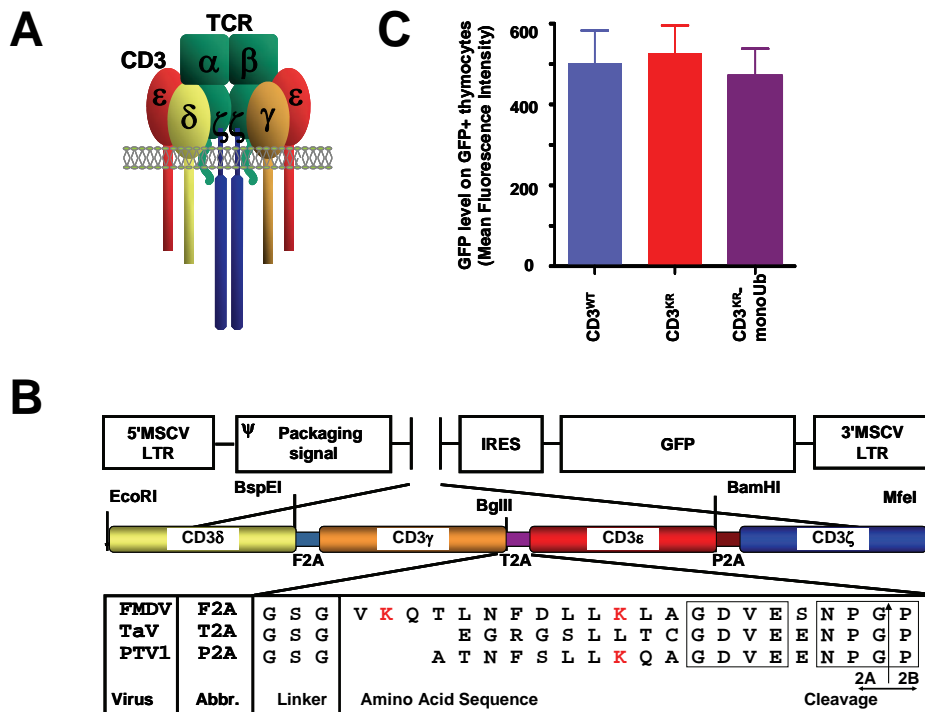


Figure S5 | Comparable retroviral transduction efficiency

(A) Schematic representation of the TCR $\alpha\beta$:CD3 $\delta\gamma\epsilon\zeta$ complex. (B) Schematic representation of the CD3-2A constructs in the MSCV-IRES-GFP (pMIG) vector as shown previously. The lysines (K) in 2A peptide are highlighted in red and are mutated to arginines to prevent ubiquitylation. (C) Retrogenic mice were generated by retroviral-mediated stem cell gene transfer using CD3 ϵ $^{-/-}$ as bone marrow donor mice and sublethally irradiated *Rag1* $^{-/-}$ as recipient mice. Thymy were isolated 5-8 weeks post bone marrow transplant. The GFP mean fluorescence intensity in GFP $^{+}$ thymocytes was measured by flow cytometry. Bars represent the mean \pm s.e.m.

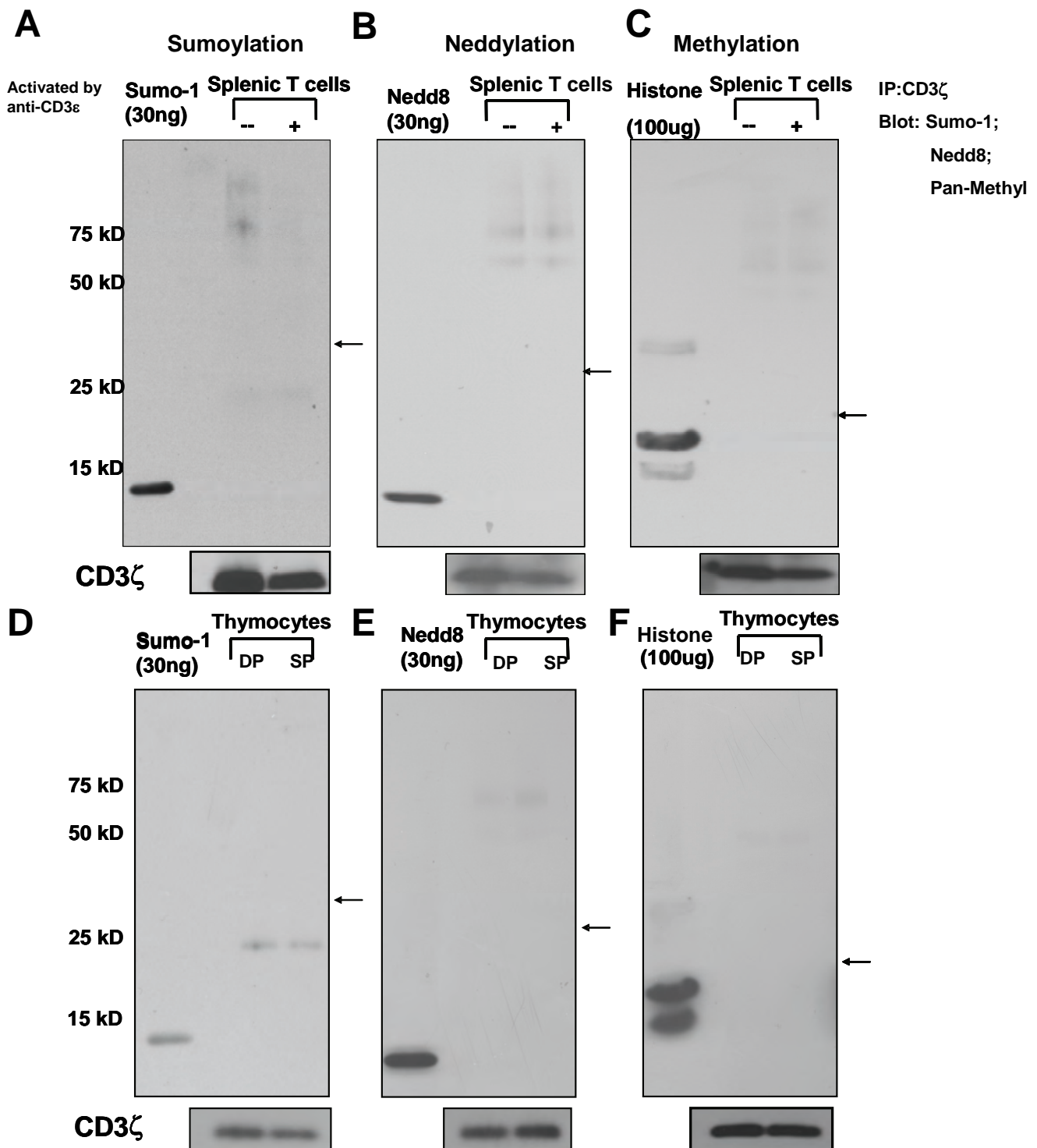


Figure S6 | No other detectable sumoylation, neddylaton, or methylation occurring on CD3 ζ

Splenic T cells were purified by MACS (A-C, 30×10^6 cells alone or activated by crosslinking with CD3 ϵ antibodies for 2 min) and SP thymocytes (D-F, 30×10^6) or DP thymocytes (D-F, 240×10^6) were purified by FACS, and lysed in 1 ml lysis buffer. The lysates were immunoprecipitated with a CD3 ζ antibody (551- ζ), separated by SDS-PAGE and Western blots probed with Sumo-1 (A and D), Nedd8 (B and E), or pan-Methyl (C and F) antibodies. Purified Sumo-1, Nedd8 and Histone proteins were loaded as positive controls. The predicted size of modified CD3 ζ is indicated by arrows. Blots were stripped and re-probed with anti-CD3 ζ (H146) to show that an equal amount of CD3 ζ was analyzed in each sample.

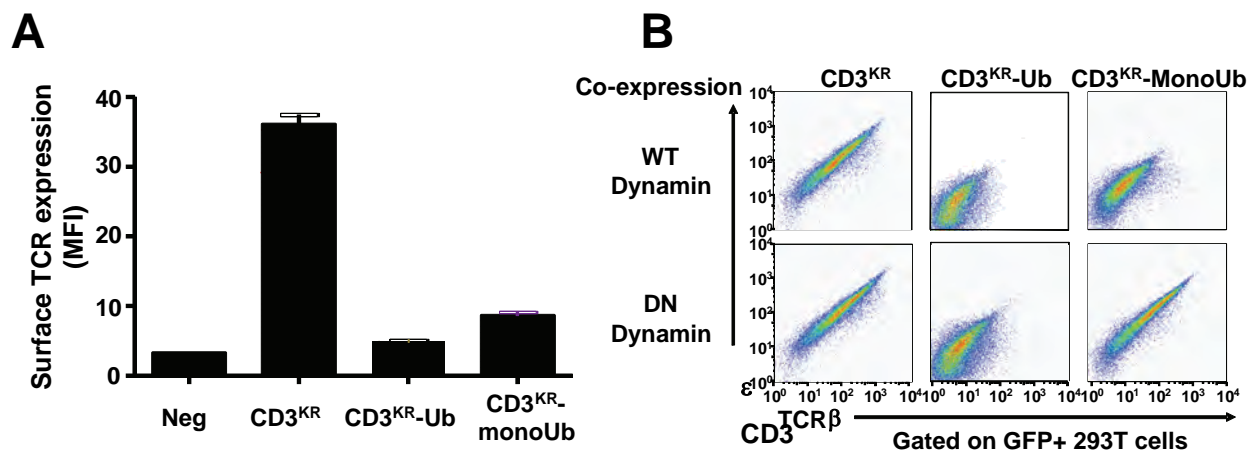


Figure S7 | Attaching mono-ubiquitin induces TCR downregulation

(A) HEK-293T cells were transiently transfected with TCR $\alpha\beta$ (2A-linked) and CD3 $\delta\gamma\epsilon\zeta$ (wild type or mutants as indicated). Transfected cells were stained with a TCR β antibody, and analyzed by flow cytometry. Bar chart shows the mean \pm s.e.m. of the TCR β mean fluorescence intensity for the GFP+ gated cell population. (B) HEK-293T cells were transfected as for (A), along with either wild type or a dominant negative dynamin. Transfected cells were stained with antibodies to CD3 ϵ and TCR β and analyzed by flow cytometry. Dot plots show the level of TCR β and CD3 ϵ surface expression for the GFP+ gated cell population.

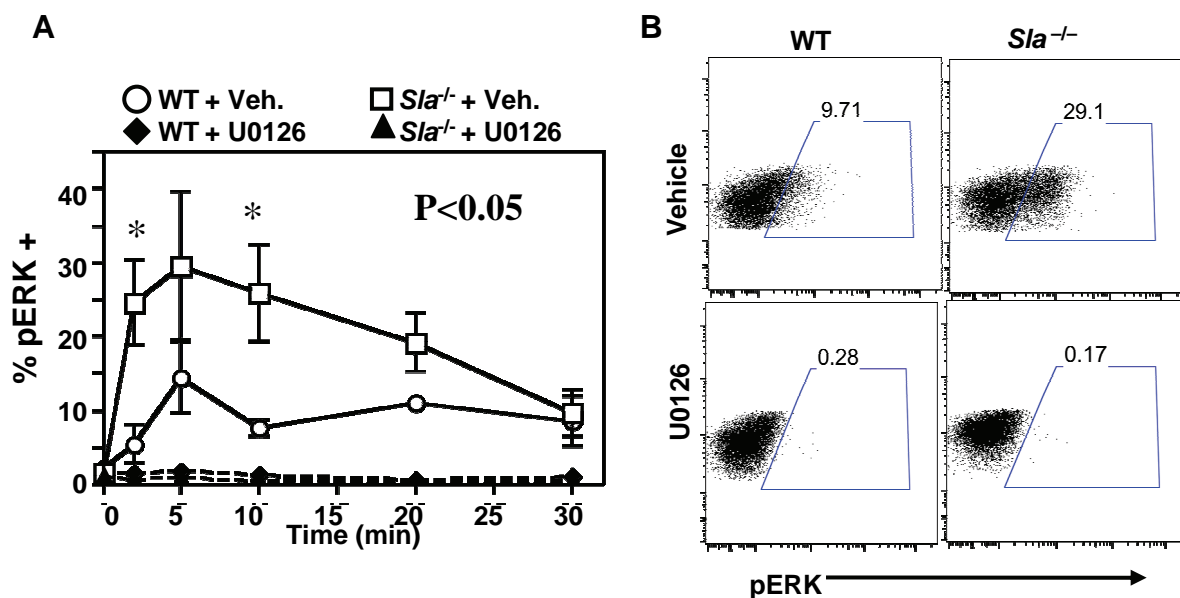


Figure S8 | Activation induced phosphorylation of ERK

Thymocytes from *Sla*^{-/-} and littermate controls were activated by crosslinking using anti-CD3 ϵ in the presence (+U0126) or absence (+Veh.) of the MEK inhibitor U0126. Thymocytes were then fixed at the indicated time, permeabilized, and stained with antibodies to CD4, CD8 and pERK. (A) CD4⁺CD8⁺ DP thymocytes were gated and pERK expression measured. (B) Representative flow cytometry dot plots are shown 10 minutes post-stimulation. Statistical significance was determined using an unpaired t test in Prism software.

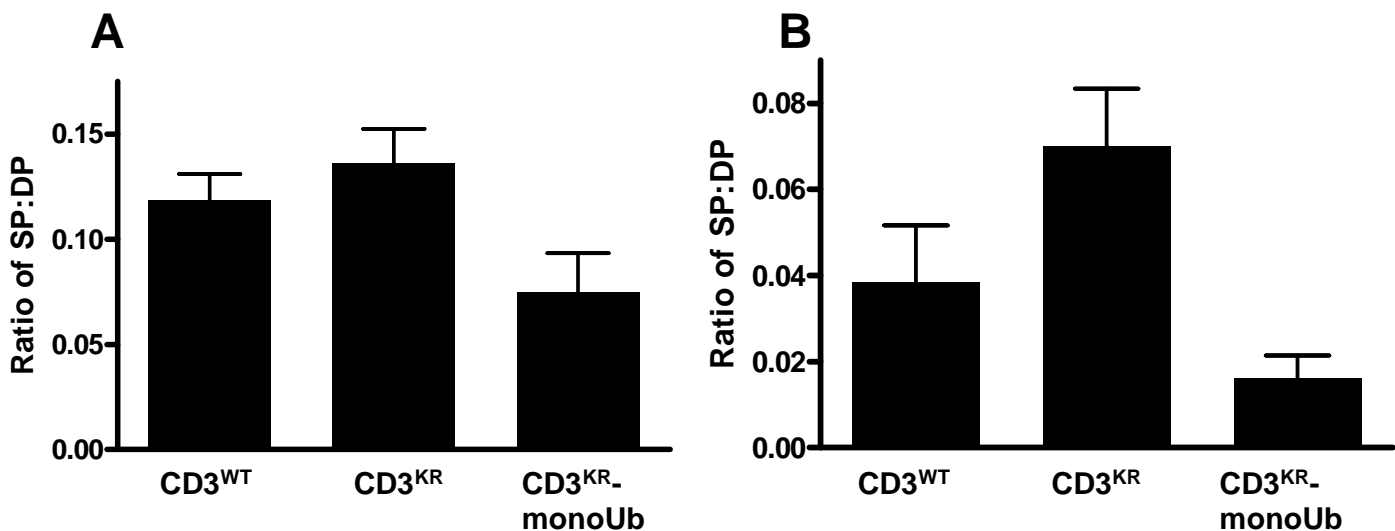


Figure S9 | Ratio of SP thymocyte number to DP thymocytes number

Retrogenic mice were generated by transducing CD3 $\epsilon\zeta$ bone marrow (A) or CD3 $\epsilon\zeta^{-/-}$ Rag1 $^{-/-}$ bone marrow (B), transplanting into sub-lethally irradiated Rag1 $^{-/-}$ recipients, and analyzing 6-8 weeks post-transfer. Thymocytes were stained with antibodies to CD4, CD8, and TCR β , and analyzed by flow cytometry. (A) The ratio of absolute numbers of SP to numbers of TCR β ⁺DP thymocytes is shown. (B) The ratio of absolute numbers of CD8 SP to numbers of TCR β ⁺DP thymocytes in female MataHari mice is shown.

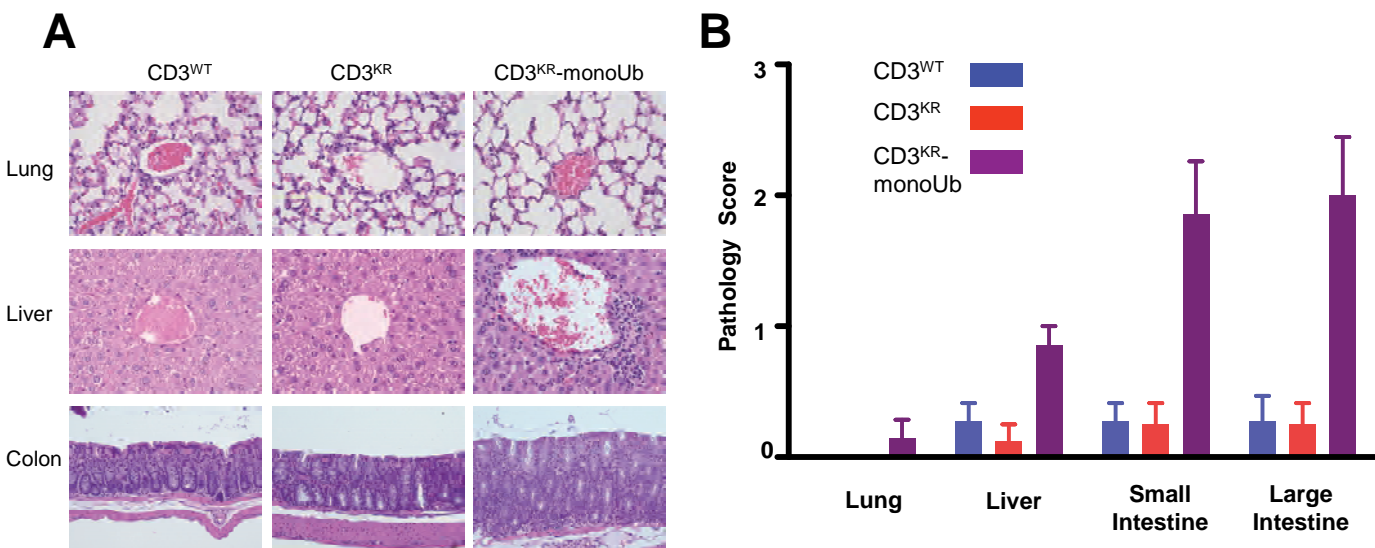


Figure S10 | Pathology of CD3^{KR}-monoUb mice

Retrogenic mice were generated reconstituting sub-lethally irradiated Rag1 $^{-/-}$ recipients with transduced CD3 $\epsilon\zeta^{-/-}$ bone marrow. Mice were sacrificed 8-12 weeks post bone marrow transfer, and the lung, liver, small and large intestine were removed for histological examination. The pathologist was blinded, and scored the level of inflammation as described in Supplementary Table 1. (A) Hematoxylin and eosin staining of formalin-fixed, paraffin-embedded sections of organs are shown. (B) Bar chart shows average pathology score of each mice group.

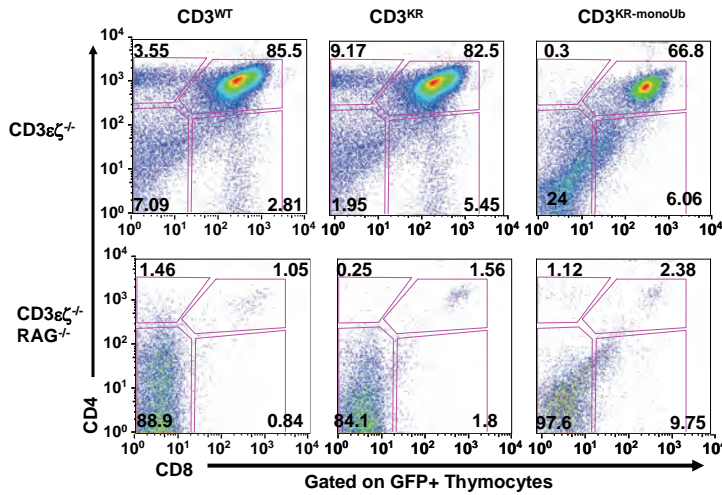


Figure S11 | Generation of DP thymocytes is blocked in absence of TCRβ.

Retrogenic mice were generated by transducing CD3εζ bone marrow (upper panel) or CD3εζ^{-/-}Rag1^{-/-} bone marrow (lower panel), transplanting into sub-lethally irradiated Rag1^{-/-} recipients, and analyzing 6-8 weeks post-transfer. Thymocytes were stained with antibodies to CD4 and CD8, and analyzed by flow cytometry.

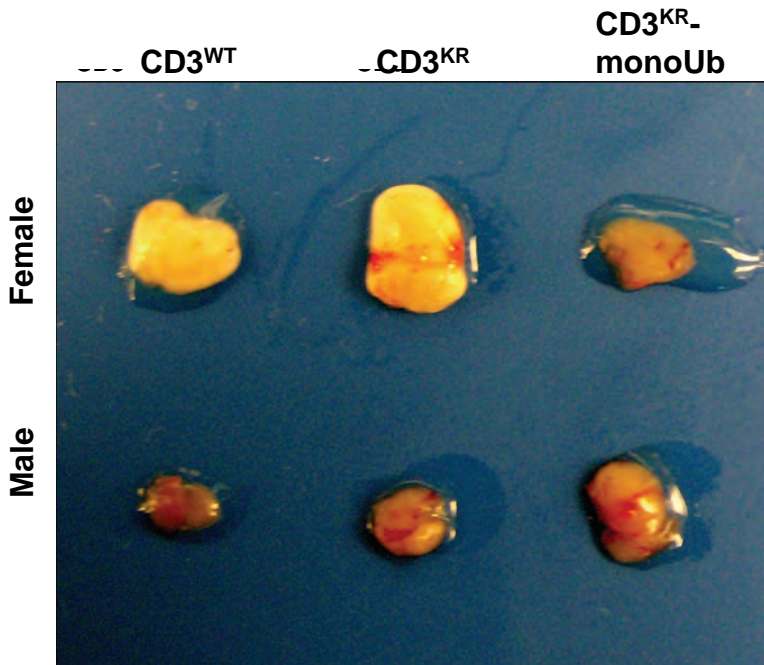
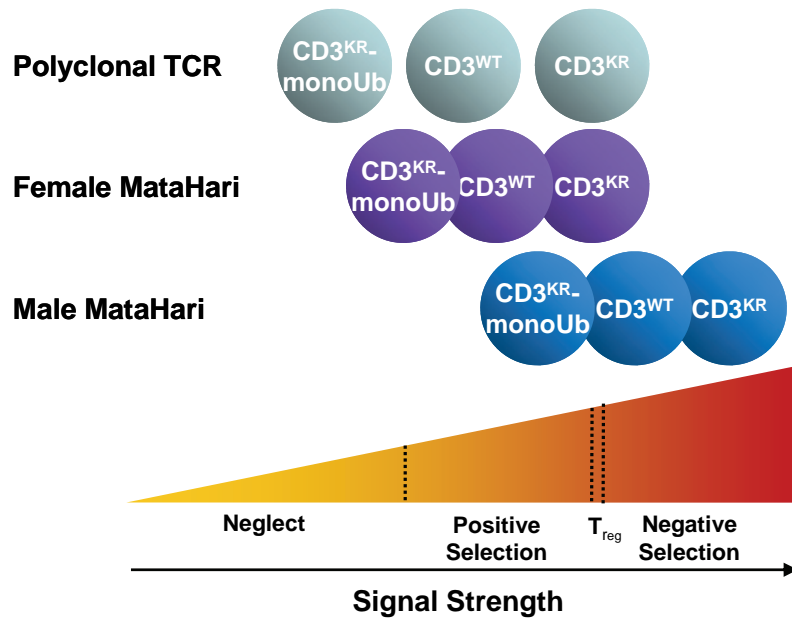


Figure S12| Thymus size of MataHari retrogenic mice

Retrogenic mice were generated by transducing CD3εζ^{-/-}Rag1^{-/-} bone marrow, transplanting into sub-lethally irradiated Rag1^{-/-} recipients, and analyzing 5-7 weeks post-transfer. Thymi were isolated and photographed to compare size of thymus.

**Figure S13| Tonic ubiquitylation and T cell development**

Schematic representation of the model: different TCR levels in the indicated retrogenic mice (CD3^{KR}>CD3^{WT}>CD3^{KR}-monoUb) alter the signal strength threshold for negative/positive selection and generation of natural T_{reg}.